ELSEVIER

Journal of Alloys and Compounds 408–412 (2006) 962–969

Journal of ALLOYS AND COMPOUNDS

www.elsevier.com/locate/jallcom

Quantitative evaluation of Ln(III) pyridine *N*-oxide carboxylic acid spectra under chemometric and metrological aspects

G. Meinrath [a,b,c,*], S. Lis [d], U. Böhme [a]

[a] *Technische Universität Bergakademie Freiberg, Institute of Inorganic Chemistry, D-09596 Freiberg, Germany*
[b] *Technische Universität Bergakademie Freiberg, Institute of Geology, D-09596 Freiberg, Germany*
[c] *RER Consultants, Schießstattweg 3a, D-94032 Passau, Germany*
[d] *A. Mickiewicz University, Department of Rare Earths, Faculty of Chemistry, Pl-60780 Poznan, Poland*

Received 26 July 2004; accepted 11 November 2004
Available online 20 June 2005

Abstract

The interaction of Nd(III) with four carboxylated pyridine *N*-oxide derivatives in aqueous solutions is studied by UV–vis absorption spectroscopy. From factor analysis in combination with computer-intensive bootstrap resampling methods the empirical probability distributions of the formation quotients of the 1:1 Nd(III) complexes with nicotinic acid *N*-oxide (**I**), picolinic acid *N*-oxide (**II**), pyridine 2,4 dicarboxylic acid *N*-oxide (**III**), and dicarboxylic acid 2,6 *N*-oxide (**IV**) are evaluated. The strength of the interaction was found to correlate with the charge density around the coordinating groups. Charge density was calculated by ab initio methods using a polarised continuum model to account for solvation effects. Evidence for a 1:2 species with **IV** is presented. A speciation diagram for this model is obtained from the probabilistic speciation code LJUNGSKILE, which visualises the rather weak evidence for a two-species system. Thus, the formation quotients $\lg \beta_{11} = 2.3 \pm 0.0_5$ (**I**), $\lg \beta_{11} = 2.7 \pm 0.0_4$ (**II**), $\lg \beta_{11} = 2.8 \pm 0.0_5$ (**III**), and $\lg \beta_{11} = 3.0 \pm 0.0_5$ (**IV**) are found to describe the chemical systems satisfactorily.

Keywords: Chemometrics; Metrology; Ab initio quantum chemical calculations; Thermodynamical data; Spectroscopy

1. Introduction

The changes in the UV–vis absorption and emission bands of lanthanide metal ions upon variation of chemical composition of the solution are interpreted by the interaction of ligands with the metal ion. The well-known Bouguer–Lambert–Beer Law provides a rational for the numerical interpretation of the experimentally observed signals. Chemometric methods allow a simultaneous numerical analysis of the digitised spectra recorded in multivariate experimental design [1,2]. The chemometric tools are continuing to grow in power and complexity.

Unfortunately, the patterns in the signals are influenced by the world surrounding the system under study. Measurements are comparisons, and only if two different comparisons are made under identical conditions, the results obtained from these both comparisons can be compared to each other [3]. Environmental influences limit the degree to which conditions can be considered to be identical. The results from each measurement itself carry limitations due to the fact that it is impossible to eliminate the undesired noise completely. Hence, in comparing the results from two measurements, it is essential to have an idea of the magnitude of the noise on the results. Even worse, the numerical methods used to analyse the patterns contribute their own bias to the results [4]. Hence, to comparatively discuss results of a study makes only sense if the reported patterns are appropriately contrasted with the noise in the data, and the bias in experiment and data evaluation. There is always the abyss of convention that prevents a clear assessment of understanding in favour of mere mutual agreement [5].

* Corresponding author. Tel.: +49 851 70372.
E-mail address: rer@panet.de (G. Meinrath).

0925-8388/$ – see front matter © 2005 Elsevier B.V. All rights reserved.
doi:10.1016/j.jallcom.2004.11.082

While exploring the absorption and luminescence properties of different pyridine *N*-oxide carboxylic acids [6–9] the question arose to which degree of certainty what statements on the speciation in solution could be made on the basis of UV–vis spectroscopic measurements. It is understood that the experimenter's ability, e.g., to control the solution composition, are limited both by the fact that each manipulation results in small variations, that instrumental operations like baseline correction introduce variation etc. Volume operations for instance were found to be approximately normally distributed with a 2% standard deviation (S.D.) from a Kolmogorov–Smirnov test from repetition studies using pipettes and a calibrated balance. It is also understood that the variations in the observed absorption spectra of lanthanide ions are weak resulting in large coefficients of correlation ρ ($\rho \sim 0.9$) [10].

2. Methodologies

The *N*-oxides of isomeric pyridine carboxylic and pyridine dicarboxylic acids were prepared from commercially available pyridine carboxylic acids (Aldrich) of highest purity and used without further purification. Details are given elsewhere [7]. Nd solutions were obtained from Nd_2O_3 produced spectroscopically pure at the Department of Rare Earth, Faculty of Chemistry, Adam Mickiewicz University, Poznan. The samples were prepared in 0.1 M perchlorate medium in volumetric flasks of 10 ml volume. Spectra were recorded from four separate runs in quartz cuvettes with 5 cm path length and averaged to reduce noise. The room temperature varied between 18 and 22 °C.

For each system, 12–15 different solution compositions were studied and simultaneously analysed. Numerical evaluations of the recorded spectra were performed by computer-assisted target factor analysis [11]. Analysis of the complete measurement uncertainty budget is performed using a threshold bootstrap scheme described previously [12,13].

With the intention to get some clues about the probable structural and electronic properties of the four ligands under study, ab initio quantum chemical calculations were performed on the B3LYP level ($6-31+G(d)$ basis set for all atoms) using the code GAUSSIAN 98 [14] with the keyword SCF = tight. The effect of solvation was accounted for by the polarised continuum model [15]. The electrostatic potentials given here are those derived from electrostatic energy surface calculations on basis of the ChelpG scheme of Wiberg et al. [16]. These calculations had the limited scope to derive some systematics in the structure and electrostatic properties of the ligand molecules. The electrostatic potentials, e.g., are not measurable but the experience shows that ab initio calculations allow to get a reasonable idea of the charge distribution within a molecule. Here, the interest is not on the absolute values for these properties but on trends in comparing these properties for several similar structures. For visualising the calculated properties the code MOLEKEL [17] was used.

3. Results and discussions

The calculated optimised solution structures with atom labelling are given in Fig. 1a (nicotinate *N*-oxid ion, **I**), Fig. 1b (picolinate *N*-oxide, **II**), Fig. 1c (pyridine 2,4 dicarboxylate *N*-oxide, **III**), and Fig. 1d (pyridine 2,6 dicarboxylate *N*-oxide, **IV**). The respective electrostatic potentials are given in Table 1.

Typically, 12–15 spectra are recorded ($^4I_{9/2} \rightarrow {}^4G_{9/2}$ transition). The molar absorption increases continuously with increasing ligand concentration. The free Nd(III) spectrum has lowest maximum absorption. The maximum amount of ligand is limited by the constraints in ionic strength. A modest bathochromic shift is observed for all four ligands. Because there is no indication that at some wavelengths only one species is absorbing exclusively, such systems can be resolved by factor analytical methods. Factor analysis is well introduced in chemistry [1,2] and no further comments will be given. A main task is the transformation of the row eigenvector matrix C^* and the column eigenvector matrix E^*, calculated by available algorithms like SVD, into physically meaningful spectra. CAT uses constraints from the experimental settings, e.g., non-negativity of absorptions and concentrations values, to optimise the target transformation matrix T in order to obtain the estimates of single component spectra in matrices E and species concentrations C according to Eq. (1). This approach is effective because T generally has a low dimensionality.

$$E^*TT^{-1}C^* = EC \quad (1)$$

Thus, sets of spectra are quickly evaluated, if the species and their stoichiometry is known. As an example, the single component spectra of the 1:1 complexes between Nd(III) and the compounds **I**, **II**, **III**, and **IV** are shown in Fig. 2. The molar absorption increases continuously from compound **I** to **IV**. In the same way, the formation quotients $\lg \beta_{11}$ calculated from the species concentration information in matrix C,

Table 1
Computed charge distribution in solvated ions **I**, **II**, **III**, and **IV**

	I	II	III	IV
1	−0.71 O	−0.72 O	−0.71 O	−0.72 O
2	0.46 N	0.43 N	0.44 N	0.37 N
3	0.92 C	1.08 C	0.87 C	1.10 C
4	−0.88 O	−0.92 O	−0.89 O	−0.93 O
5	−0.88 O	−0.92 O	−0.88 O	−0.92 O
6	−0.06 C	−0.12 C	0.06 C	−0.10 C
7	−0.08 C	−0.06 C	1.09 C	1.08 C
8	0.14 H	0.14 H	−0.93 O	−0.92 O
9	−0.11 C	−0.13 C	−0.92 O	−0.93 O
10	0.13 H	0.14 H	−0.12 C	−0.10 C
11	−0.11 C	−0.06 C	−0.18 C	−0.15 C
12	0.14 H	0.13 H	0.13 H	0.13 H
13	−0.12 C	−0.15 C	−0.19 C	0.03 C
14	0.15 H	0.15 H	0.16 H	0.13 H
15			−0.05 C	−0.16 C
16			0.16 H	0.13 H

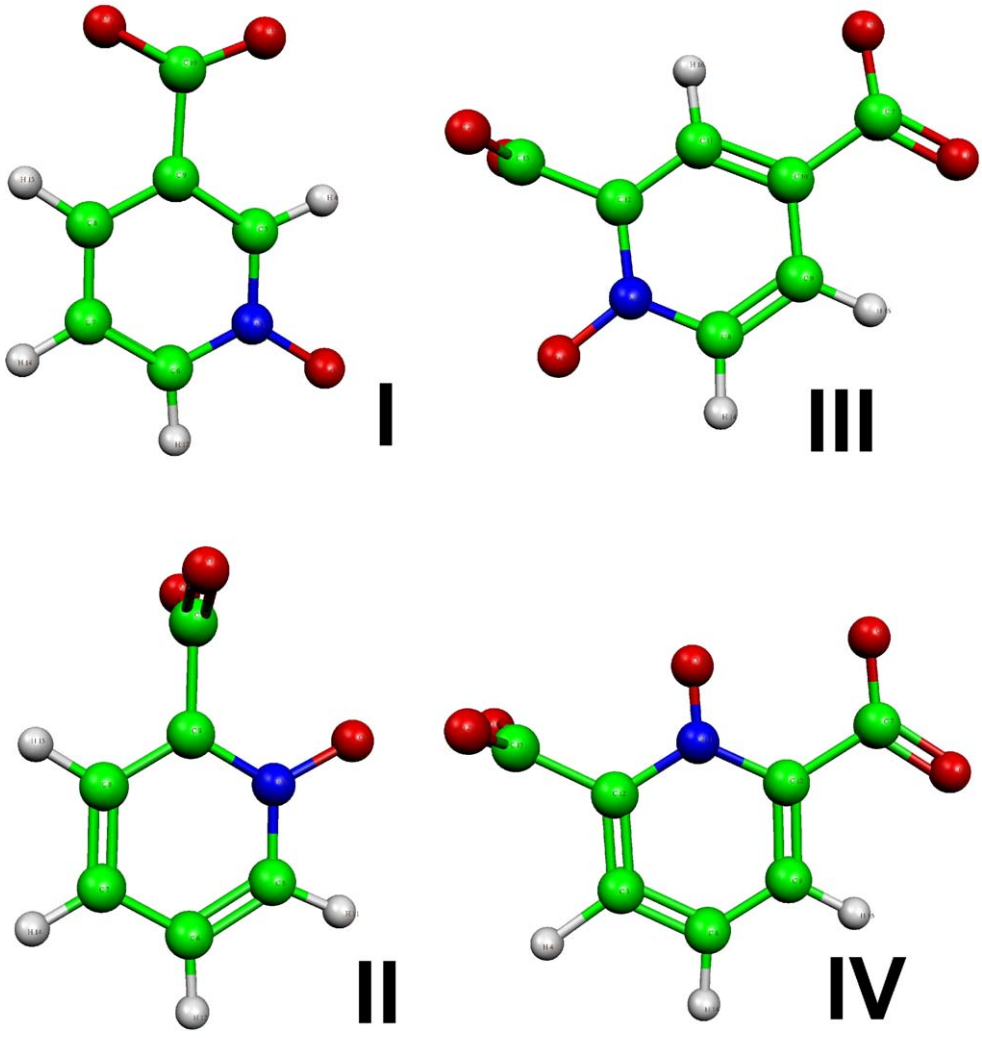

Fig. 1. Ball-and-stick representations of the ligands nicotinate *N*-oxide (**I**), picolinate *N*-oxide (**II**), pyridine 2,4 dicarboxylate *N*-oxide (**III**), and pyridine 2,6 dicarboxylate *N*-oxide (dipyr 2,6 NO) (**IV**). The structures are optimised by ab initio calculations in aqueous solution using a polarised continuum model. The atom labels correspond to the labels given in Table 1.

increase accordingly as shown in Table 2. Also included in Table 2 are the computed dipole moments and group charge densities of the carboxylate (**I**) and carboxylate NO group (**II**, **III**, and **IV**).

It is obvious that the dipole moment alone is not a good criterion to judge coordination strength, even though interaction between lanthanide ion and ligand is considered to be predominantly ionic while covalent contributions are almost negligible. Using the computed electrostatic potentials, however, shows that the carboxyl group in I, being unassisted by a neighbouring NO group, has a considerably weaker electrostatic potential compared to those compounds with

Table 2
Thermodynamical properties of ligands **I**, **II**, **III**, and **IV** in aqueous solution calculated by quantum-chemical methods and formation quotients lg β_{11} of the interaction for the 1:1 complex of these ligands with Nd(III) from spectroscopic measurements evaluated by CAT

Ligand	lg β_{11}	lg β_{11} (TB CAT)[a]	Dipole moment (D)[b]	Charge densities[c]
I	2.31 ± 0.13	2.31 **2.37** 2.41	14.8	−0.844 (−0.844)
II	2.64 ± 0.11	2.67 **2.71** 2.74	16.3	−1.047 (−1.473)
III	2.78 ± 0.09	2.72 **2.81** 2.86	8.55	−1.029 (−1.466)
IV	2.86 ± 0.20	2.90 **2.96** 3.00	15.9	−1.105 (−1.478)

[a] Bold figure gives the median, l.h.s. values gives lower, r.h.s. values upper 0.68 percentile limits from the empirical probability distribution obtained by 2000 TB CAT cycles.
[b] Calculated from Gaussian 98 at the B3LYP level using a PCM solvent model for water.
[c] Calculated from the SCF densities using the CHelpG approach; the largest charge density of the carboxyl group is given, while data in brackets give the sum of the carboxyl group and the neighbouring N–O group where applicable.

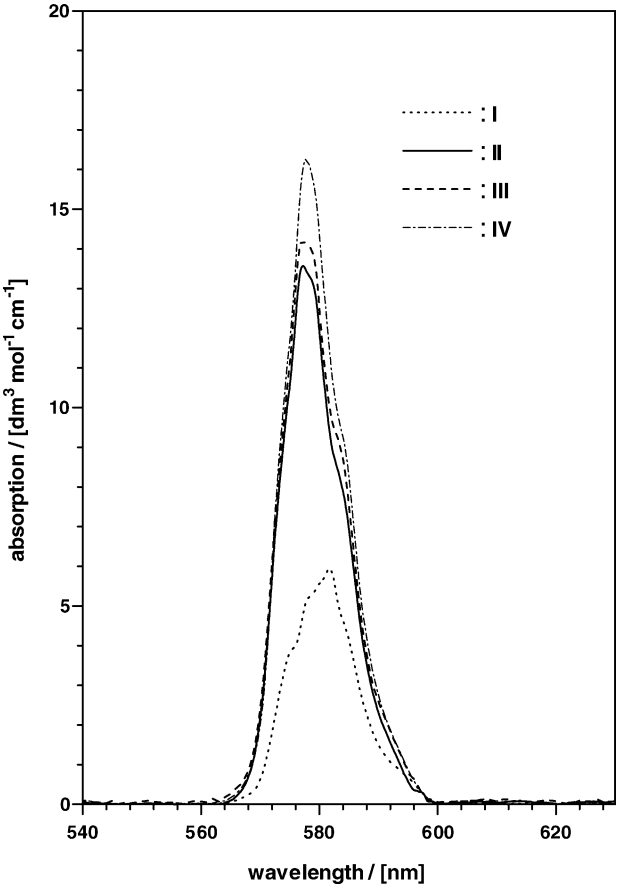

Fig. 2. Single component spectra of the 1:1 species of Nd(III) with the ligands **I**, **II**, **III**, and **IV**. The spectra are evaluated from single CAT runs. Mean values are given.

a neighbouring NO group. A linear trend analysis of the formation constants as a function of the carboxylate charge densities even results in a reasonable Pearson coefficient of correlation $r = -0.95$; a parameter which is often mistakenly reported as measure of goodness of fit. The correlation indicates that some common trend is to be found in the evaluated formation quotients and the electrostatic potentials.

The spectroscopic information can be analysed on several levels. First, factor analysis is used to evaluate single component spectra and formation quotients from the available experimental data. For each sample holding a species in appropriate amounts, one formation quotient will be obtained. This approach is classical. Its results will be critically discussed and the rational for the more complex threshold bootstrap approach will emerge.

3.1. Classical approach: mean value-oriented evaluation

CAT evaluates a formation constant for each solution where the concentration of educts and products are satisfying the physical constraints and some statistical significance criterion based on the Clifford's multivariate method [18]. Such preliminary statistical analysis avoids to include spurious data into the output data. The evaluated formation quotients are then pooled to obtain a mean value and a S.D. in a classical way. The resulting mean values together with the S.D.s are given in the second column of Table 2.

The classical approach does have its limitations. Clearly, a mean value-based analysis is ignoring information in the CAT output asking for caution in the data interpretation. For illustration, non-normal distribution of the observed formation quotients, outliers in the spectral data and outlier(s) in the samples can be mentioned. Classical, mean value based factor analytical methods give no hint.

A second caveat comes from the fact that only one possible interpretation has been considered, namely the formation of a 1:1 complex for all four ligands. Previous researchers claim formation of 1:1 and 1:2 complexes between lanthanides and picolinic acid *N*-oxide (**II**) [19]. From that study, a $\beta_{11} = 2.91$ is reported from pH titration in 2.0 M perchlorate medium. It is not possible to make a comment on this previous work, because no estimate of uncertainty has been given. Like all other methods, pH titrations are affected by a series of influences, which cannot be controlled by the experimenter with arbitrary accuracy. Hence it remains unclear to what degree the experimental variance attributed to the 1:2 complex was statistically significant. It is understood that computational capabilities in the mid-60s were very limited, but today these questions nevertheless arise. Judging values without meaningful estimate of uncertainty is metrologically unacceptable.

3.2. Complete uncertainty budget approach: threshold bootstrap

Likewise, spectroscopic studies are affected by several factors limiting our capabilities in recognising the information about the investigated chemical systems. Table 3 gives a list of these measurement uncertainties and the type of contribution they make. Random contributions must be taken into account in the evaluation procedure. Bias, however, must be avoided or at least minimised by the experimenter. If the bias can be quantified, it is sometimes possible to correct for. In the present study, three random effects are considered by normal distributions: relative uncertainty in the metal ion concentration of 4%, relative uncertainty in the ligand concentration of 7% and a relative uncertainty in each volume operation by 2%. Other random contributions have a marginal magnitude. The major contribution to the measurement uncertainty budget, however, must be accounted for by more complex statistical procedures. These effects are correlation in the residuals, correlation in the spectra, non-normality and non-linearity. Further contributions are the statistical optimisation criterion, the weighing scheme and Monte-Carlo effects. Here, computer-intensive resampling schemes have been made available in recent years allowing to incorporate statistical analysis into complex data evaluation procedures [20]. Threshold bootstrap is a self-adaptive resampling scheme which requires the CAT procedure to be repeated a larger number of times, e.g., 1000–2000 repeti-

Table 3
Causes and type of measurement uncertainties considered by TB CAT

Cause	Contribution	Type of contribution
Metal ion concentration	Purity of compound	Bias
	Concentration of stock solution	Random
	Accuracy/precision of volumetric operations	Random
	Accuracy/precision of balance	Random
Ligand concentration	Purity of compound	Bias
	Concentration of stock solution	Random
	Accuracy/precision of volumetric operations	Random
	Stability of solution (e.g., photodegradation)	Random
	Accuracy/precision of balance	Random
Spectrometer settings	Slit width	Bias
	Averaging	Bias
	Repeatability	Random
	Wavelengths stability	Random
	Scan speed/attenuation	Random
	Background noise	Random
Cuvette cells	Path length	Systematic
	Difference sample cell/blank cell	Systematic
	Colloidal effects	Random
	Stray light	Systematic
	Dust	Random
	Photodegradation	Random/ systematic
Temperature		Random
Ionic strength		Random

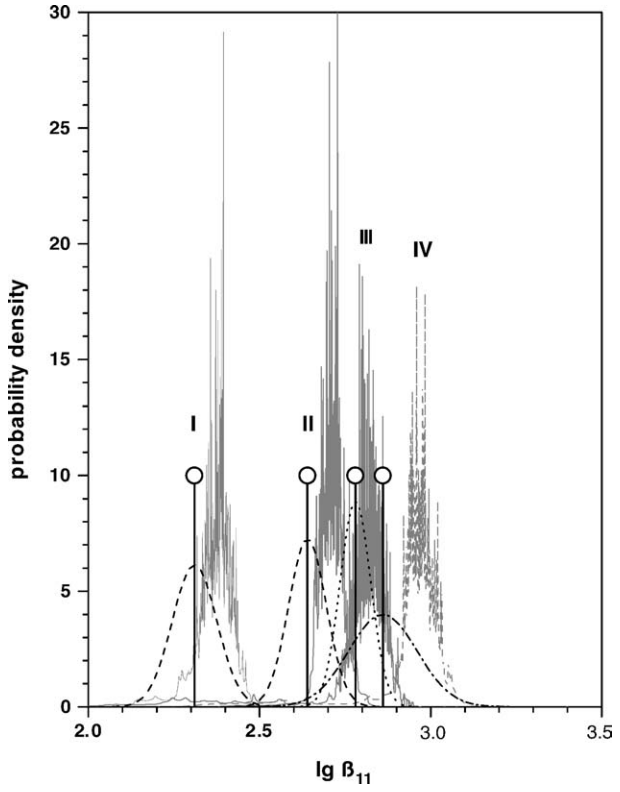

Fig. 3. A comparison of the probability densities of the quantity lg β_{11} from 2000 TB CAT cycles with mean values (circles with drop values) and normal probability density estimates (dashed gaussian curves) for the 1:1 species of Nd(III) with ligands **I**, **II**, **III**, and **IV**. In the single CAT runs, measurement uncertainties were not included. The gaussian curves represent merely the variability of calculated lg β_{11} within the 12 sample solutions. The TB CAT derived probability densities include measurement uncertainties and correlation effects (cf. Table 1).

tions. In each repetition, the spectra are contaminated with some noise in a defined way, while the other input quantities, e.g., concentrations are modified randomly according to the above given relative uncertainties, and the analysis is repeated. From the formation constants evaluated in each of the repetitions, the empirical distribution of the formation constants is evaluated. A result is shown in Fig. 3, where the empirical distributions for the 1:1 model are contrasted with normal distributions representing the mean values and S.D.s obtained from a single CAT run in Table 2.

Fig. 3 gives a justification for the TB CAT procedure. The single run mean values, indicated in Fig. 3 by a circle with a drop line, are mostly at the lower edge of the empirical distribution as obtained by 2000 TB CAT cycles. Only by including the S.D., a reasonable overlap of the both distributions evaluated for each species can be observed.

The discussion of results up to now assumes that the solution chemistry can be reasonably described by the formation of a 1:1 complex between Nd(III) and the ligand. Are there other interpretations possible, which may describe the solution behaviour more adequately? The properties of the systems holding ligands **II** and **III** have been discussed previously [9,10]. In both cases, no explanation of the spectral information on basis of a two species system was possible.

The pyridine 2,6 dicarboxylic acid ligand (**IV**) shows a high charge density over the CO_2–NO–CO_2-group with its doubly negative charge. Therefore, it may be argued that its tendency to coordinate with formally singly charged $[Nd(dipyr\ 2,6\ NO)]^+$ species is higher compared to ligands **II** and **III**. In fact, an analysis by TB CAT gives three different acceptable parameter combinations resulting in a chemical system with two coordinated species. The distribution of the formation constants lg β_{11} and lg β_{12} for the $[Nd(dipyr\ 2,6\ NO)]^+$ species and the $[Nd(dipyr\ 26\ NO)_2]^-$ species, respectively, are shown in Fig. 4. The three different solutions will be termed A, B, and C, respectively.

Solution A produces two broad distributions, where the distribution ($A_{1:2}$) is continuously distributed between $3 < \lg \beta_{12} < 8$. A closer inspection of the evaluated single component spectra shows that both spectra are almost identical. The solutions B and C, however, look reasonable. Solution B has the median values lg $\beta_{11} = 3.1$ and $\beta_{12} = 7.1$. Solution C gives lg $\beta_{11} = 3.6$ and lg $\beta_{12} = 5.4$. While there is

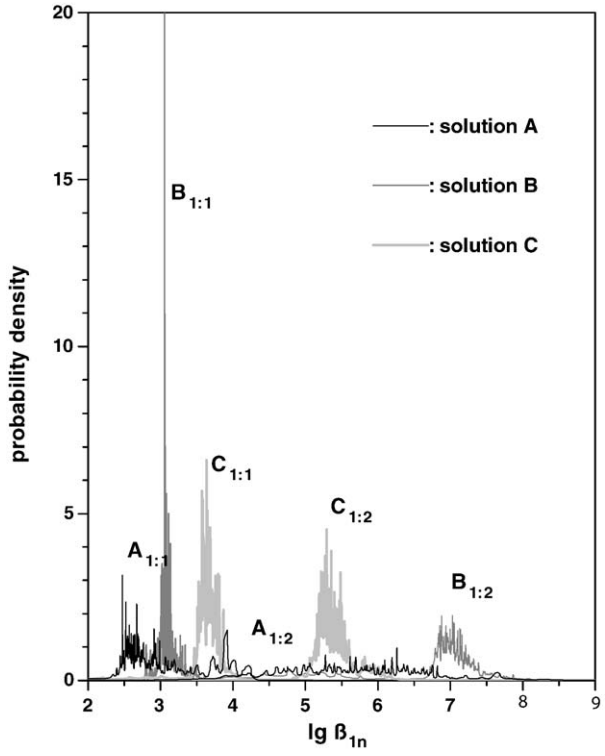

Fig. 4. Comparison of probability densities for the quantities $\lg \beta_{11}$ and $\lg \beta_{12}$ of the Nd(III) interaction with **IV**. Three different numerical solutions were found to interpret the spectral data. Only solution C is acceptable under physically and chemical aspects.

no reason to assume a stepwise formation constant $\lg K_{12}$

$$\lg K_{12} = \lg \beta_{12} - \lg \beta_{11} \quad (2)$$

to be larger than $\lg \beta_{11}$ in case of solution B, the formation constants obtained for solution C look reasonable. With the intention to visualise the solution composition, a speciation diagram calculated on basis of the formation constants for solution C is given in Fig. 5. Because a mere mean value based speciation would fail to transport the limitations in the interpretation of the system, the speciation diagram in Fig. 5 is calculated with the probabilistic speciation code LJUNGSKILE [21]. LJUNGSKILE uses Latin hypercube sampling (LHS) schemes to evaluate the impact of uncertainties in modelling parameters on the model output. The formation quotients applied in the calculation are $\lg \beta_{11} = 3.6 \pm 0.3$ and $\lg \beta_{12} = 5.5 \pm 0.3$. These values were derived from a Kolmogorov–Smirnov analysis of the empirical cumulative distributions. Kolmogorov–Smirnov test gave a probability below 0.1% that the empirical distribution curves are normally distributed.

Fig. 5 is derived from 64 runs at each interval. Ligand concentration intervals are 0.0003 mol dm^{-3}. Total Nd(III) concentration is 0.005 mol dm^{-3}. The abscissa axis is the total ligand concentration, while the solution species Nd^{3+}, $Nd(dipyr\ 26\ NO)^{+}$, $Nd(dipyr\ 26\ NO)_2^{-}$, and $(dipyr\ 26\ NO)^{2-}$ are given in the graph. From the 64 LHS runs an empirical distribution curve is evaluated at each interval. Form this

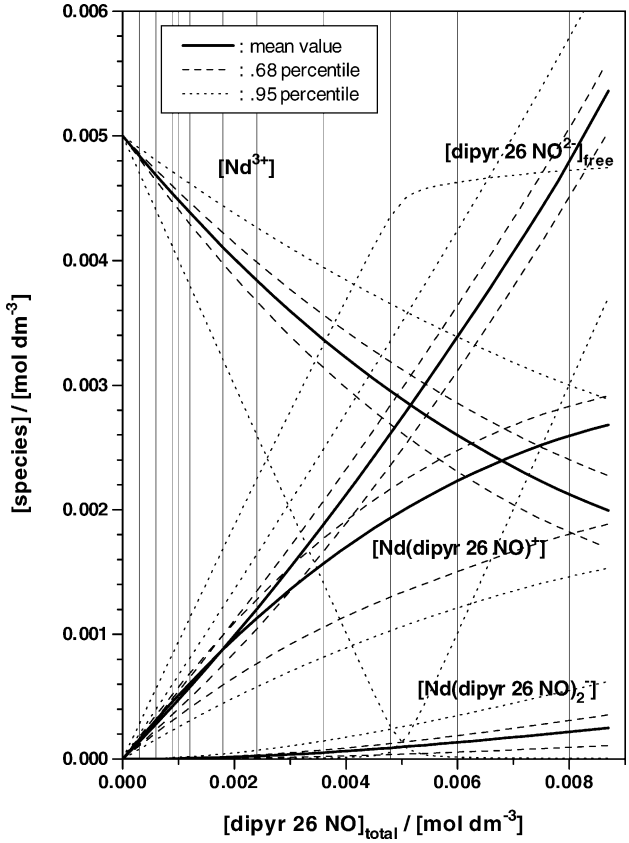

Fig. 5. Speciation diagram of Nd(III) with ligand **IV** including 68 and 95% confidence limits for the species Nd^{3+}, $Nd(dipyr\ 26\ NO)^{+}$, $Nd(dipyr\ 26\ NO)_2^{-}$, and (dipyr 26 NO) free as a function of the total (dipyr 26 NO) concentration. The lines indicate ligand concentrations where spectra have been recorded. The species concentrations are obtained from 64 LHS cycles by the probabilistic speciation code LJUNGSKILE on basis of formation quotients of solution C (cf. Fig. 4). The diagram shows that predicted concentrations of the 1:2 species $Nd(dipyr\ 26\ NO)_2^{-}$ are rather low even at the highest total ligand concentration and insignificant compared to the uncertainties.

empirical distribution, Fig. 5 shows the median (solid lines), the 0.68 percentile (dashed lines), and the 0.95 percentiles (dotted lines) for each species.

From an inspection of Fig. 5 it becomes evident that a study of solutions with higher ligand concentrations might not necessarily improve the information to be extracted from the data set. Due to the mutual correlation in the spectral information [10,12] the uncertainty range increases with increasing ligand concentration, while the concentration of the $Nd(dipyr\ 26\ NO)_2^{-}$ is increasing only slightly. Despite the fact that Fig. 5 is derived on basis of data obtained under the assumption that a 1:2 species exists, the concentration of this species are not significant on the 95% confidence level because the lower 0.95 percentile limit is always below zero. Hence, evidence for the presence of a 1:2 complex may be accepted on the 68% level but not on the 95% confidence level. The presence of a 1:2 complex seems the more doubtful when comparing the formation constant $\lg \beta_{11}$ with those obtained for the 1:1 species of ligands **I**, **II**, and **III**. For the latter complexes $\lg \beta_{11}$ is of the order 2.3–2.7. For ligand **IV**, the

respective value is about one order of magnitude higher if the spectral data is interpreted by two coordinated species.

4. Conclusions

The data evaluation allows to state with some confidence that the NO group significantly enhances the affinity of the respective ligands towards Nd(III) in aqueous solution. The interaction of **I** with Nd(III) is significantly less than the interaction of **II**. There is no indication that nicotinate *N*-oxide (**I**) or picolinate *N*-oxide might form a 1:2 species under the conditions applied in this study. Therefore, the probability distributions for ligands **I** and **II** in Fig. 4 reflect the thermodynamic situation for the both systems. For the picolinate *N*-oxide system, previous researchers speculated on the formation of distinct five-member or six-member rings in the coordination of picolinate and picolinate *N*-oxide to the lanthanide ions. Planar molecules were assumed and differences in the formation quotients were explained by different stabilities in the different ring sizes. The ab initio calculations performed in this study indicate an additional option. Because the carboxylate group may rotate freely, it will be repulsed by the negatively polarised *N*-oxide group. The calculated dihedral angle between the plane of the pyridine ring and the carboxyl group in an aqueous solvent is 91.8°. There is only one single crystal structure of a lanthanide picolinic acid *N*-oxide compound, 6-methylpicolinic acid *N*-oxide with lanthanum(III) [22] where unfortunately dihedral angles are not given. The graphical display of the molecular structure, however, indicates that the carboxyl group is not in plane with the methylated pyridine ring, too.

Ab initio calculations in combination with a polarised continuum model for the ligand molecules in aqueous solution have provided helpful insight into the trends in the electrostatic behaviour. These calculations should be considered in that way: indicating trends. There is no claim that the calculations performed during this study are of highest accuracy. While the absolute values should be treated with cautions, the qualitative trends are reflected in the evaluated data, e.g., the maximum molar absorptions of the coordinated species and the formation quotients.

The analysis of the Nd(III) dipyr 26 NO (**IV**) interaction revealed some faint evidence for formation of a 1:2 species. TB CAT is designed to test alternative models. From the three different possible numerical solutions for such a model, only one was found to be of relevance. The probabilistic speciation code LJUNGSKILE was applied to simulate the likely composition of the sample solutions under these model constraints. The concentrations of a 1:2 species were found at the limits given the applied analytical and numerical tools. Extending the experimental range to higher ligand concentrations was found unlikely to produce clearer evidence. Hence, a solution system involving formation of a 1:2 species was rejected. It should be emphasised that the uncertainty in the species Nd^{3+} and the 1:1 species $Nd(dipyr\,26\,NO)^{+}$ are higher than the predicted total concentration of the 1:2 species. Hence, no claim is made that the 1:2 species does not exist. The resolution power of the experimental method is not high enough to provide clear evidence to support claims for its existence.

Each operation in the preparation of the Nd stock solution, e.g., dissolving the solid Nd_2O_3, weighing, preparing aliquots etc. introduces some deviation. It is probably that the true Nd(III) concentration is, say $0.0047\,mol\,dm^{-3}$ or $0.0054\,mol\,dm^{-3}$. Any attempt to reproduce this study at a different location and a different time will have to cope with the same measurement uncertainty. Limitations in the analytical methods are evident from measurement evaluation programs of the EU, e.g., [23] and the key comparison exercises of the BIPM, e.g., [24]. ISO's Guide to the Expression of Uncertainty in Measurement (GUM) [25] provides an internationally accepted convention for the evaluation of reasonable, meaningful and traceable uncertainty limits. This study provides an example for the application of the GUM concepts in the evaluation of complex chemical measurements and the interpretation of the obtained numerical data by probabilistic decision tools like the LJUNGSKILE code [26].

References

[1] R. Malinowski, Factor Analysis in Chemistry, third ed., Wiley Interscience, New York/USA, 1995, 351.
[2] M. Otto, Chemometrics, Wiley-VCH, Weinheim/D, 2002.
[3] S. Ellison, W. Wegscheider, A. Williams, Anal. Chem. 69 (1997) 607A–613A.
[4] I.E. Frank, J.H. Friedman, Technometrics 35 (1993) 109.
[5] G. Price, Measurement 29 (2001) 293–305.
[6] S. Lis, Z. Hnatejko, S. But, A. Szyczewski, M. Elbanowski, Mol. Phys. 101 (2003) 977–981.
[7] S. Lis, Z. Hnatejko, P. Barczynski, M. Elbanowski, J. Alloy Comp. 344 (2002) 70–75.
[8] S. Lis, Z. Hnatejko, S. But, A. Szyczewski, M. Elbanowski, Mol. Phys. 101 (2003) 977–981.
[9] G. Meinrath, Z. Hnatejko, S. Lis, Talanta 63 (2004) 287–296.
[10] G. Meinrath, S. Lis, Z. Piskula, Anal. Bioanal. Chem. 378 (2004) 221–226.
[11] G. Meinrath, S. Lis, Fresenius J. Anal. Chem. 369 (2001) 124–133.
[12] G. Meinrath, Anal. Chim. Acta 415 (2000) 105–115.
[13] G. Meinrath, S. Lis, Anal. Bioanal. Chem. 372 (2002) 333–340.
[14] M.J. Frisch, G.W. Trucks, H.B. Schlegel, G.E. Scuseria, M.A. Robb, J.R. Cheeseman, V.G. Zakrzewski, J.A. Montgomery, Jr., R.E. Stratmann, J.C. Burant, S. Dapprich, J.M. Millam, A.D. Daniels, K.N. Kudin, M.C. Strain, O. Farkas, J. Tomasi, V. Barone, M. Cossi, R. Cammi, B. Mennucci, C. Pomelli, C. Adamo, S. Clifford, J. Ochterski, G.A. Petersson, P.Y. Ayala, Q. Cui, K. Morokuma, D.K. Malick, A.D. Rabuck, K. Raghavachari, J.B. Foresman, J. Cioslowski, J.V. Ortiz, A.G. Baboul, B.B. Stefanov, G. Liu, A. Liashenko, P. Piskorz, I. Komaromi, R. Gomperts, R.L. Martin, D.J. Fox, T. Keith, M.A. Al-Laham, C.Y. Peng, A. Nanayakkara, C. Gonzalez, M. Challacombe, P.M.W. Gill, B. Johnson, W. Chen, M.W. Wong, J.L. Andres, C. Gonzalez, M. Head-Gordon, E.S. Replogle, J.A. Pople, GAUSSIAN 98. Revision A 7. Gaussian Inc. Pittsburgh.
[15] S. Miertus, J. Tomasi, Chem. Phys. 65 (1982) 239.
[16] K.B. Wiberg, C.M. Hadad, T.J. LePage, C.M. Breneman, M.J. Frisch, J. Phys. Chem. 96 (1992) 671.

[17] P. Flükiger, H.P. Lüthi, S. Portmann. Molekel 4.3. Swiss Centre for Scientific Computing. Manno/CH (2000–2002).
[18] A.A. Clifford, Multivariate Error Analysis, Applied Science, London/UK, 1973.
[19] H. Yoneda, G.R. Choppin, J.L. Bear, A.J. Graffeo, Inorg. Chem. 5 (1965) 244–246.
[20] B. Efron, SIAM Rev. 21 (1979) 460–480.
[21] A. Ödegaard-Jensen, C. Ekberg, G. Meinrath, Talanta 63 (2004) 907–916.
[22] L. Yan, J. Liu, X. Wang, R. Yang, F. Song, Polyhedron 14 (1995) 3545–3548.
[23] Y. Aregbe, C. Harper, J. Norgaard, M. de Smet, P. Smeyers, L. Van Nevel, Ph.D.P. Taylor, Accred. Qual. Assur. 9 (2004) 323–332.
[24] http://www.bipm.fr/kcdb/.
[25] ISO, Guide to the expression of uncertainty in measurement. Second ed. ISO, Geneva/CH (1995).
[26] A. Ödegaard-Jensen, C. Ekberg, G. Meinrath, Mat. Res. Soc. Symp. 757 (2003) 509–514.